[Soviet Phys. Solid State 11, 1448 (1970)].
[13]I. L. Spain, J. Chem. Phys. 52, 2763 (1970).
[14]J. W. McClure, in Proceedings of the Conference on the Physics of Semimetals and Narrow Gap Semiconductors, Dallas, Texas, 1970 (unpublished); J. Phys. Chem. Solids (to be published).
[15]G. Wagoner, Phys. Rev. 118, 647 (1960).
[16]J. A. Woollam, Phys. Rev. Letters 25, 810 (1970).
[17]E. N. Adams and T. D. Holstein, J. Phys. Chem. Solids 10, 254 (1959).
[18]K. Sugihara and S. Ono, J. Phys. Soc. Japan 21, 631 (1966).
[19]J. A. Woollam, Phys. Rev. 185, 995 (1969), and references therein.
[20]J. M. Ziman, *Electrons and Phonons* (Oxford U. P., Oxford, England, 1962).
[21]J. W. McClure and W. J. Spry, Phys. Rev. 165, 809 (1968).
[22]P. B. Horton, Ph. D. thesis, Louisiana State University, 1964 (unpublished).
[23]G. Fair and P. Taylor, Bull. Am. Phys. Soc. 15, 1252 (1970); and H. J. Trodahl (unpublished).
[24]H. G. Callen, Phys. Rev. 73, 1349 (1948).
[25]D. K. C. MacDonald, *Thermoelectricity* (Wiley, New York, 1962), p. 11.
[26]Y. N. Obraztsov, Fiz. Tverd. Tela 7, 455 (1965) [Soviet Phys. Solid State 7, 573 (1965)].
[27]P. S. Zyrganov and Kalashnikov, Fiz. Metal. i Metalloved. 18, 166 (1964).
[28]K. D. Tsêndin and A. L. Éfros, Fiz. Tverd. Tela 8, 306 (1966) [Soviet Phys. Solid State 8, 378 (1966)].
[29]I. M. Lifshitz and A. M. Kosevich, Zh. Eksperim. i Teor. Fiz. 29, 730 (1956) [Soviet Phys. JETP 2, 636 (1956)].
[30]R. B. Dingle, Proc. Roy. Soc. (London) A211, 517 (1952).
[31]J. W. McClure, Phys. Rev. 119, 606 (1960).
[32]J. W. McClure, Phys. Rev. 108, 612 (1957).
[33]J. W. McClure, IBM J. Res. Develop. 8, 255 (1964).
[34]P. R. Schroeder, M. S. Dresselhaus, and A. Javan, in Conference on the Physics of Semimetals and Narrow Gap Semiconductors, Dallas, Texas, 1970 (unpublished); J. Phys. Chem. Solids (to be published).
[35]J. A. Woollam (unpublished).
[36]M. Inoue, J. Phys. Soc. Japan 17, 808 (1962).
[37]J. C. Laurence, NASA Report No. TN D-4910, 1968 (unpublished).
[38]J. A. Woollam, Rev. Sci. Instr. 41, 284 (1970).
[39]J. R. Long, C. G. Grenier, and J. M. Reynolds, Phys. Rev. 140, A187 (1965).

PHYSICAL REVIEW B VOLUME 3, NUMBER 4 15 FEBRUARY 1971

Polarization Effects in the Electroreflectance of Bismuth Telluride at Oblique Incidence*

A. Balzarotti
Istituto di Fisica dell'Università di Roma, Roma, Italy

and

E. Burattini and P. Picozzi
Istituto di Fisica dell'Università dell'Aquila, Aquila, Italy

(Received 3 August 1970)

The optical transitions above the threshold of the uniaxial crystal bismuth telluride have been investigated by means of electroreflectance over the energy range 1–5.5 eV using an electrolyte to produce electric fields at the surface. Both near-normal and oblique incidence measurements were made using light polarized under different orientations of the electric vector with respect to the c axis. The combination of these techniques permitted an unambiguous identification of the symmetry of the critical points and yielded the precise polarization dependence of the transitions. The broad electroreflectance spectra of bismuth telluride have been understood and analyzed in terms of strongly lifetime-broadened Franz-Keldysh tunneling. A correlation, although preliminary, has been attempted with the band structure of this material.

I. INTRODUCTION

Recent theoretical and experimental papers have raised new interest in the optical properties of bismuth telluride and of other rhombohedral crystals of the homologous group, bismuth selenide and antimony telluride.

Besides the early work of Lee and Pincherle,[1] based upon an augmented-plane-wave (APW) calculation of the band structure of bismuth telluride, two more theoretical works appeared which made use of the pseudopotential approach. Borghese and Donato[2] have evaluated the band structure of bismuth telluride at the high-symmetry points of the Brillouin zone including the spin-orbit interaction, and have tried to interpret the reflectivity spectra of Greenaway and Harbeke[3] and to check the galvanomagnetic data of various authors. Their results agree with the six-valley model for both conduction and valence bands,[4–7] but their interpretation of the high-energy optical transitions differs remarkably from that given by Greenaway and Harbeke.

More recently Katsuki[8] calculated the band energy also along lower-symmetry lines and on the reflec-

tion planes near the extrema of the conduction and the valence bands. His results are also consistent with some galvanomagnetic experiments,[9,10] but do not touch upon the interpretation of the optical data.

On the other hand, the up-to-date experimental knowledge of the optical transitions of bismuth telluride comes from the above-mentioned experiment of Greenaway and Harbeke and from that of Sobolev *et al.*,[11] which looked at the reflectivity of this compound up to 12 eV. Although general agreement exists on the energy position of the more pronounced peaks of this compound, it seems that the structure is more complex than reported in Ref. 3. Moreover, the polarization dependence of the peak intensities and positions is still more doubtful.

The electroreflectance (ER) experiments to be reported in this paper aimed at a detailed investigation of the optical transitions of energy higher than the indirect edge of bismuth telluride, and their dependence on the polarization of light. This latter point is particularly important in anisotropic crystals because different selection rules for optical transitions are effective depending upon whether the electric vector of the light is parallel or perpendicular to the direction of their c axis.

The ER measurements were taken both at nearly normal incidence and at several angles near the pseudo-Brewster angle φ_B using light linearly polarized in the plane of incidence or normally to it.

A description of the experimental technique is given in Sec. II and the results of measurements at normal and oblique incidence are presented in Secs. III A and III B, respectively. Section IV is devoted to the discussion of these results, while an attempt is made in Sec. V to correlate the ER transitions to the available band structure.

II. EXPERIMENT

The modulated reflectance coefficient was measured by reflecting the light upon the (111) surfaces, which are the planes of easy cleavage perpendicular to the c axis. After each series of measurements the reflecting surfaces were renewed by cleaving the specimens with self-adhesive tape. Due to the large anisotropy of bismuth telluride, these surfaces were mirrorlike and no further etching treatment was necessary to improve their optical quality.

All the samples were p-type single crystals with an electrical resistivity at room temperature of about 0.003 Ω cm and a positive thermoelectric power $\alpha \cong 250\ \mu V/\text{deg}$. This relatively high thermoelectric power implied that our samples were not degenerate and indicated[12] that the Fermi level lay about 0.03 eV above the top of the valence band. The corresponding hole concentration[13] was $p = 2 \times 10^{18}\ \text{cm}^{-3}$, taking for the hole effective mass the value[14] $m_h = 0.46 m_0$, where m_0 is the free-electron mass.

The modulation was applied by the electrolytic technique[15] using a 1-molar solution of KCl in water or methanol. The samples were immersed in the solution at the center of a semicylindrical quartz cell such that the incident- and the reflected-light beams propagated in the radial direction without undergoing refraction from the glass walls of the cell and from the solution. This arrangement permitted us to carry out measurements at grazing incidence and avoided the restrictions due to the limit angle of the glass-air system. Both the cell and the detector were placed on a goniometer and carefully shielded from external light.

The experimental apparatus was of a standard type for this kind of measurement. The optical assembly consisted of a stabilized tungsten or deuterium lamp, a Beckmann model DU monochromator and a glan-air polarizer mounted in front of the sample and capable of rotation about its axis. Both a photomultiplier (RCA 1P 28) and a CdSe photoresistance were employed to cover the spectral range 1–5 eV. The ac signal was synchronously processed by a PAR model JB-4 phase-lock amplifier synchronized at the field frequency, while the dc output of the detector was kept constant throughout the entire spectral range by a servomechanism acting on the width of the exit slit of the monochromator and driven by a feedback signal proportional to the anode current of the photomultiplier. The output of the lock-in amplifier, which is directly proportional to the relative change of the reflectivity $\Delta R/R$ induced by the electric field, was continuously recorded on an x-y plotter, whose x axis was driven by the scanning mechanism of the monochromator.

A very accurate focusing procedure was adopted to minimize light losses due to the limited surface of the samples, especially at high incidence angles. Owing to the weak reactivity of bismuth telluride with the solution, the surface remained clean for long periods of time assuring good reproducibility of the measurements.

III. RESULTS

A. ER at Near-Normal Incidence

Several near-normal ER spectra were taken at different modulation voltages not exceeding $3V_{pp}$, where pp means peak to peak. Figure 1 shows a typical spectrum obtained for $V_{ac} = 2V_{pp}$ and $V_{dc} = 0$.[16] The general shapes and locations of the structures are practically not modified by changes in the driving voltage, provided that the modulating field is not too large. At high modulation levels ($> 5\ V_{pp}$) the voltage waveform begins to distort due to conduction effects taking place in the electrolyte. In small gap semiconductors excessive modulation voltages can easily drive the surface to degeneracy. In these conditions the spectral line shape should strongly depend on the

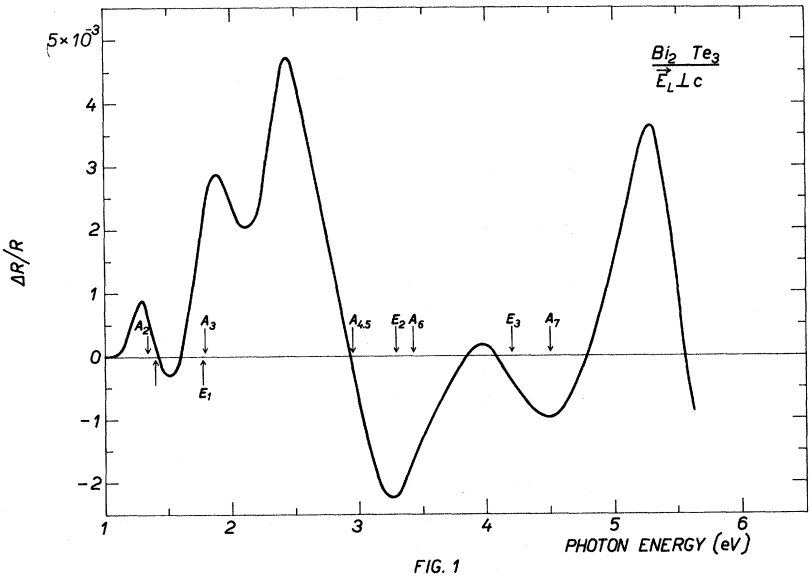

FIG. 1

FIG. 1. ER of Bi_2Te_3 for a (111) face at near-normal incidence in the fundamental absorption region ($V_{ac}=2\ V_{pp}$, $V_{dc}=0$). The arrows locate the energies of the transitions as identified in Refs. 3 and 11.

field strength because of the field inhomogeneity[17] within the space-charge region. We found that, at sufficiently low modulation levels, and no dc bias, the line shapes of Fig. 1 were nearly independent on the applied voltage and the ER signal did not change sign, indicating that the surface inversion could not be reached. This behavior suggests that the field inhomogeneity at the surface is sufficiently small to be neglected and therefore the uniform field approximation seems applicable in these experimental conditions. It should, however, be noted that the large broadening effects present in the ER spectra of this compound could mask the line-shape evolution at moderate field strengths.

We wish also to remark that large contributions to the ER spectra resulting from changes of the optical constants of the electrolyte[18] can surely be excluded in this wavelength range since similar results were obtained with different electrolytic solutions.

In Fig. 1 the positions of peaks and shoulders seen in absolute reflectivity are labeled with the same symbols as used by the authors. A refers to the measurements of Sobolev *et al.*, while E refers to those of Greenaway and Harbeke.

The ER spectrum does not consist of sharp lines located at each of the critical points (cp) as in the case of a typical Franz-Keldysh response, but rather consists of broadened structures covering wide energy ranges. It is, however, apparent from Fig. 1 that some correspondence exists between the transitions of the absolute reflectance and the large oscillations in ER, with a possible exception of the A_6 and/or E_2 lines. The transition which gives rise to the large positive peak at 5.3 eV of the differential spectrum was not detected in absolute reflectance, even at low temperature, but it clearly appears as a peak at about 5.7 eV in the energy-loss function $-\mathrm{Im}(1/\tilde{\epsilon})$.[3]

In order to correlate the ER to the cp, the modulated reflectance $\Delta R/R$ was subjected to the Kramers-Kronig transformation, which gives the corresponding change $\Delta\chi$ in the phase angle. This quantity is related to $\Delta\tilde{r}/\tilde{r}$, the relative change in the complex reflection coefficient $\tilde{r}=R^{1/2}e^{i\chi}$, through the relation

$$\Delta\tilde{r}/\tilde{r}=\tfrac{1}{2}\,(\Delta R/R)+i\Delta\chi\,, \tag{1}$$

where

$$\Delta\tilde{r}/\tilde{r}=[n\tilde{\epsilon}^{-1/2}/(\tilde{\epsilon}-n^2)]\,d\tilde{\epsilon}\,. \tag{2}$$

In Eq. (2) $\tilde{\epsilon}=\epsilon_1+i\epsilon_2$ represents the complex dielectric constant of the material and n is the (real) refractive index of the first medium.

For sake of comparison, the values of $\tilde{\epsilon}$ appearing in Eq. (2) were derived from the reflectivity data of Refs. 3 and 11 through a Kramers-Kronig analysis.[19] While the results of Ref. 3 are well reproduced, the lower reflectance of Sobolev *et al.* gives consistently smaller values for the optical constants. Due to the closer agreement with the measured values of the long-wavelength refractive index,[20] the room-temperature reflectivity of Greenaway and Harbeke was considered as more reliable in the low-energy region and the corresponding optical constants were used in all the following calculations.

Figure 2 shows $\Delta\epsilon_1$ and $\Delta\epsilon_2$ calculated from the data of Fig. 1. A main difference between the $\Delta R/R$

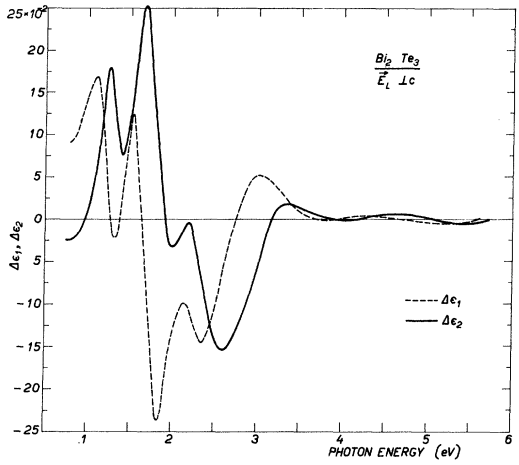

FIG. 2. Field-induced change of the real (dashed) and imaginary (solid) parts of dielectric constant (from data of Fig. 1).

curve and the field-induced change $\tilde{\epsilon}(F) - \tilde{\epsilon}(0)$ is found for the low-energy transitions which are greatly enhanced after the Kramers-Kronig transformation with respect to the high-energy structures.

In the presence of large broadening effects the overlapping of the individual contributions is considerable and the energy locations of the cp together with their identification cannot be established without a careful line-shape analysis.

In Sec. IV we intend to show quantitatively that both A_2 and A_3 singularities correspond to M_1 longitudinal saddle-point edges, while $A_{4,5}$ is due to an M_0 edge. No attempt is made to identify the remaining transitions at higher energies because their contribution to the $\Delta\tilde{\epsilon}$ spectrum is too weak for a positive identification; therefore their energy location in Table I should be considered as approximate.

B. ER at Oblique Incidence

The possibility of gaining further insight on the ER response is offered by measurements at nonnormal incidence for angles near the pseudo-Brewster angle and light polarized in the plane of incidence. The method was first emphasized by Fischer and Seraphin[21] and also considered experimentally.[22–25] The power of the method arises from the fact that each type of cp exhibits a peculiar angular line shape for the parallel component of the ER $(\Delta R/R)_p$ and it is therefore possible to take advantage of this to characterize the nature of the singularity involved. The strong line-shape changes near the Brewster angle for fixed polarization (parallel to the plane of incidence) and modulation determine the spectral behavior of the entire ER spectrum.

We present in Fig. 3 the parallel component of the ER measured at various angles near the pseudo-Brewster minimum as a function of photon energy up to 3 eV. The following features should be stressed:

(i) The first peak at 1.3 eV grows continuously with increasing angle of incidence up to 80° and then decreases, shifting slightly towards high energies.

(ii) The weak transition near 2 eV vanishes at large angles. This behavior together with the fact that it is always present in the perpendicular component $(\Delta R/R)_s$ even at grazing incidence, strongly suggests that it should be allowed only for $\vec{E}_L \perp c$.

(iii) The positive wing associated with the next transition gradually increases and shifts to high energies and then decreases and moves back towards its initial position.

It is worthwhile noting here that the growth and decay of the peaks is consistent with the expected dependence of the Brewster angle φ_B upon the wavelength.[26]

Before proceeding to a detailed analysis of the

TABLE I. Energy positions (in eV) of the main optical transitions of Bi_2Te_3. Data from the present experiment are included for comparison with those of the reflectivity measurements.

Transitions	A_1	A_2	$A_3(E_1)$	$A_{4,5}$	(E_2)	A_6	$A_7(E_3)$	A_7'
R[a] (295 °K)	•••	1.36	1.80	2.95	•••	3.4	4.5	•••
R[a] (90 °K)	•••	1.36	1.80	2.90	•••	3.4	4.5	•••
R[b] (300 °K)	0.3	•••	1.78	•••	3.23	•••	4.2	•••
R[b] (77°K)	0.3	1.4	•••	•••	•••	•••	•••	•••
ϵ_2[c]	0.5	•••	1.7	2.7	•••	•••	4.0	5.6[d]
ϵ_2[e]	0.5	1.3	1.6	•••	2.7	•••	•••	5.7[d]
$\Delta\epsilon_2$	•••	1.3	1.76	2.5	•••	•••	4.2	5.7
Γ	•••	0.26	0.3	0.6	•••	•••	•••	•••
Type	•••	$M_{1\parallel}$	$M_{1\parallel}$	M_0	•••	•••	•••	•••

[a]From Ref. 11.
[b]From Ref. 3.
[c]Calculated from Ref. 11.
[d]Calculated from the energy-loss function.
[e]Calculated from Ref. 3.

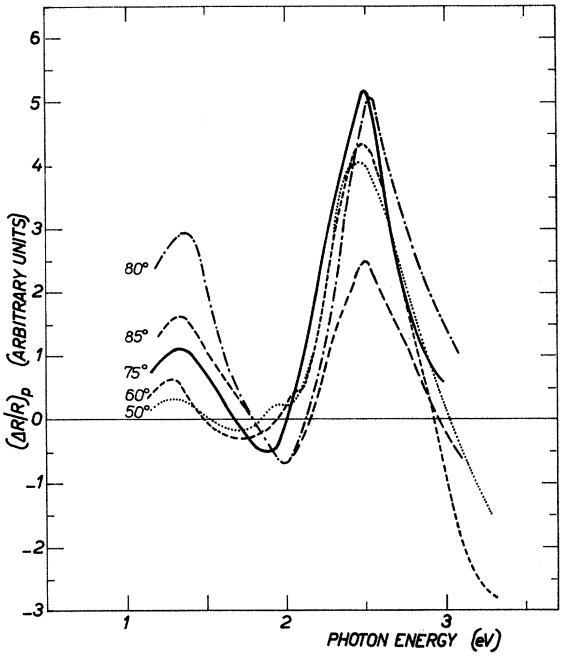

FIG. 3. Parallel component of the ER of bismuth telluride at oblique incidence.

polarization results, we wish to remark that the exact understanding of the angular dependence of the line shape of the ER can only be achieved when the separate contributions to the ER response have been recognized and this requires a preliminary theoretical analysis of the lines which will be carried out in Sec. IV.

IV. DISCUSSION

As mentioned in Sec. III A, the ER of bismuth telluride is characterized by broad structures extending over a few electron volts, a feature which is common to the electro-optic response of lead salts[27] and of other materials having large static dielectric constants.[28]

In the presence of broad structures it is necessary to introduce the lifetime-broadened electro-optical functions F and G in order to account for the experimental results. The general expressions for these functions have been given by Aspnes[29] in terms of Airy functions of a complex variable and of their derivatives. The relaxation constant Γ appears in the complex argument of the Airy function

$$z = x_0 + i\,\Gamma/\Theta = \pm\,(\omega_c - \omega)/\Theta + i\,\Gamma/\Theta\,,$$

where $\hbar\omega_c$ is the critical point energy and $\Theta = (q^2 F^2/2\mu\hbar)^{1/3}$. The field-induced changes of the complex dielectric function at all cp can be written

$$\Delta\tilde{\epsilon} = \pm\frac{B\Theta^{1/2}K}{\omega^2}\,H^{\pm}\left(x_0,\ \frac{\Gamma}{\Theta}\right), \qquad (3)$$

where $H^{\pm}(x_0,\ \Gamma/\Theta) = F(x_0,\ \Gamma/\Theta) \pm iG(x_0,\ \Gamma/\Theta)$ and $K = 1$ or i, according as the electro-optic responses of an M_1 and M_2 or of the other cp are needed. The choice of the signs in Eq. (3) appropriate to the various cases is given in Ref. 29.

We have analyzed the results of Fig. 1 by assuming that the experimental $\Delta R/R$ up to 3.5 eV can be accounted for by the ER of just three cp. The low-energy side of the spectrum, below 2.5 eV, is well reproduced by the ER of a pair of M_1 longitudinal saddle-point edges with the symmetry axis of odd-sign mass aligned parallel to the electric field (and, therefore, to the c axis). An M_0 threshold is a good candidate to explain the high-energy side of the spectrum. We have attempted to fit the experimental data by overlapping the contributions of the two M_1 saddle points located at 1.3 and 1.76 eV, and of the M_0 singularity at 2.5 eV. The results of this analysis are shown in Fig. 4 and compared with the experimental data (triangles) of Fig. 1. The actual magnitude of the theoretical ER depends upon the value of the dipole matrix element between the initial and final states of the transition [included in the B coefficient of Eq. (3)] which is generally unknown, so the theoretical curve has been arbitrarily normalized to the experiment at 1.55 eV where the contribution of the A_3 transition is dominant. The relaxation constants used in the calculations have been summarized in Table I. The reduced effective masses of the A_2, A_3, and $A_{4,5}$ cp are found to be in

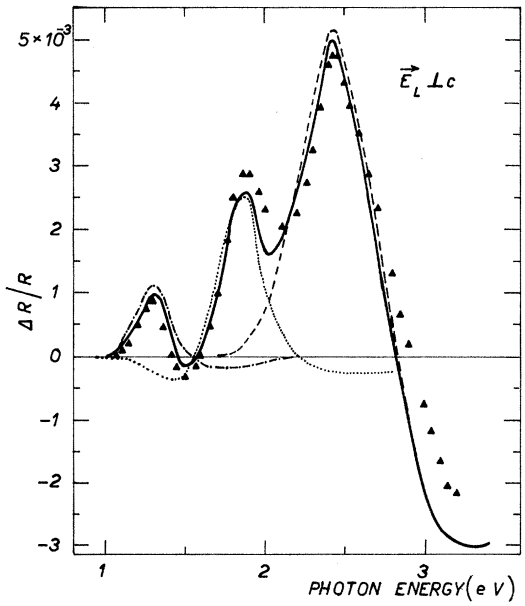

FIG. 4. Experimental (triangles) and theoretical (solid line) changes of reflectance ($\vec{E}_L \perp c$) due to an M_0 threshold at 2.5 eV and two $M_{1\parallel}$ saddle-point edges at 1.3 eV and 1.76 eV. The dashed curves are the individual contributions of the cp.

the ratios $m_1 : m_2 : m_3 = 2:1:0.25$.

A further confirmation of the correctness of our preceding identification is provided by the dependence of the peak intensities and positions on the polarization of the light. The M_1 saddle-point line shape $(\Delta R/R)_p$ at 1.3 eV is characterized by a positive peak which grows to a maximum till 80° and then decreases. The low-energy negative peak increases continuously till 85°, giving to the whole structure a symmetrical aspect. The parabolic case consists of a dispersionlike structure at normal incidence which evolves into a single peak with small satellites on both energy sides. A continuous "blue" shift of the whole structure in both cases is also present.

All these features should be recovered in the calculated spectrum of Fig. 5 which includes the overlapping contribution of all three cp. Comparison with the curves of Fig. 3 immediately shows that the low-energy experimental line shape is not well reproduced theoretically. In particular, the intermediate transition increases towards grazing incidence while the positive peak of the A_2 transition decreases at angles larger than 75° in contrast with the experiment.

The agreement between theory and experiment improves considerably if we assume that the A_3 transition is strongly polarization dependent and forbidden for $\vec{E}_L \parallel c$. The effect of canceling the contribution of the intermediate transition on the ER spectrum of Fig. 5 is shown in Fig. 6. The agreement is quite good for large incidence angles and deteriorates (as expected) going towards normal incidence when the weight of the $A_3(E_1)$ transition

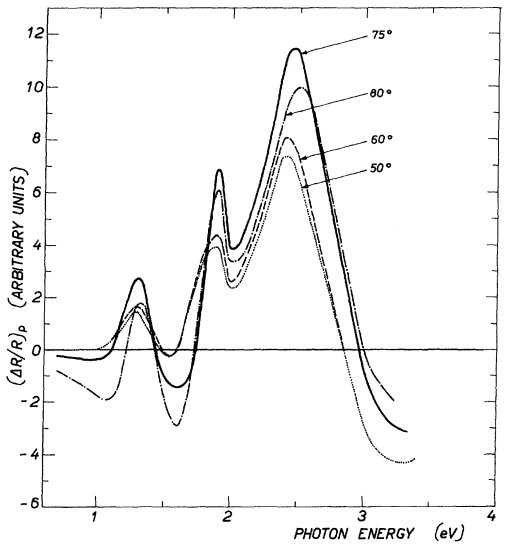

FIG. 5. Calculated line shapes of $(\Delta R/R)_p$ for different angles of incidence near the pseudo-Brewster angle.

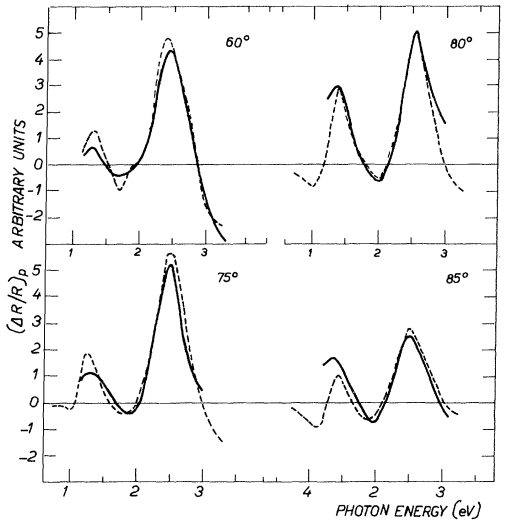

FIG. 6. Comparison between the experimental $(\Delta R/R)_p$ curves of Fig. 3 (solid lines) and the theoretical lines calculated under the assumption that the A_3 transition (1.76 eV) is forbidden for $\vec{E}_L \parallel c$ (dashed lines).

can no longer be neglected. It is therefore apparent that the A_3 transition is allowed only for $\vec{E}_L \perp c$, while the remaining transitions are probably allowed for both the polarization directions.

The dependence of $A_3(E_1)$ on the polarization agrees with the conclusions of Ref. 3, while for A_2 and E_2 structures we obtain different results. Owing to the possibility that the E_2 transition corresponds[11] to A_6 or to a superposition of two neighboring $A_{4,5}$ and A_6 peaks, the polarization dependence of the E_2 transition reported in Ref. 3 is questionable. In this case the nonoccurrence of the A_6 transition in the differential spectrum might not be surprising if we consider that, according to Eq. (3), structures with large broadening parameters Γ/Θ dominate and nearby transitions due to cp with large masses could be almost completely masked. Furthermore, it should be considered, as already pointed out in Ref. 3, that reflectivity data taken on cleaved surfaces are difficult to compare with those from polished and etched surfaces. In the case of anisotropic samples, when weak polarization effects are to be detected, oblique measurements are generally to be preferred.

In the case of light polarized perpendicularly to the plane of incidence, the three peaks of Fig. 3 decrease continuously with increasing angle of incidence and do not shift in energy. This behavior, which follows the monotone decrease of the Seraphin coefficients α and β with the incidence angle, is also well accounted theoretically.

With regard to the results of Figs. 5 and 6, we wish to remark that in the calculated line shapes no account was taken of the possible anisotropy of the

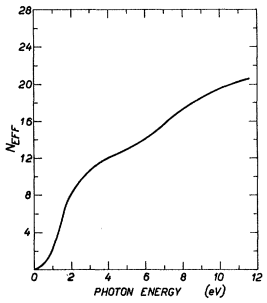

FIG. 7. Effective number of electrons per unit cell vs photon energy.

complex dielectric constant. This approximation, which may be too drastic if applied to strongly anisotropic crystals (for instance, graphite[30]), seems to hold here for bismuth telluride, at least within the accuracy required by the present analysis.[31]

V. BAND STRUCTURE OF BISMUTH TELLURIDE

The outer electronic configuration of the bismuth atom is $6s^26p^3$, while the tellurium is $5s^25p^4$, giving 28 electrons per unit cell to be accomodated in the different valence bands. The valence states of bismuth telluride consist of two groups of bands, well separated in energy, from which originate the transitions to the lowest p-like conduction band states responsible for the two series of peaks observed in the reflectivity.[3,11] This picture is further supported by the dependence of the effective number of electrons in the unit cell n_{eff} contributing to the optical transitions. This quantity is given by the sum rule

$$n_{eff}(\omega_0) = \frac{mV}{2\pi^2 e^2} \int_0^{\omega_0} \omega \epsilon_2(\omega)\, d\omega \,, \tag{4}$$

where $V = 173\,\text{Å}^3$ is the volume of the unit cell of bismuth telluride. We have calculated n_{eff} as a function of photon energy from Eq. (4) and the result is shown in Fig. 7.

N_{eff} rises rapidly at low energies and then starts to saturate at about 14 electrons around 6 eV. This rise is associated with the onset of interband transitions starting from the first six or seven valence bands of the upper group. The next transitions, originating from the deeper valence states, take place at still higher energies and cause n_{eff} to rise again.

The upper set of bands has a prevalent p character while the lower group of bands should have predominatly s-like symmetry. As a matter of fact, the replacement of Bi atoms in the crystals with lighter Sb atoms yields larger changes in the energy of the high reflectivity peaks with respect to the low-energy transitions. This behavior, which is common to the PbTe-SnTe-GeTe family,[32] is caused by the stronger relativistic corrections on the s-like valence states.[11] With decreasing atomic number, the energy of the

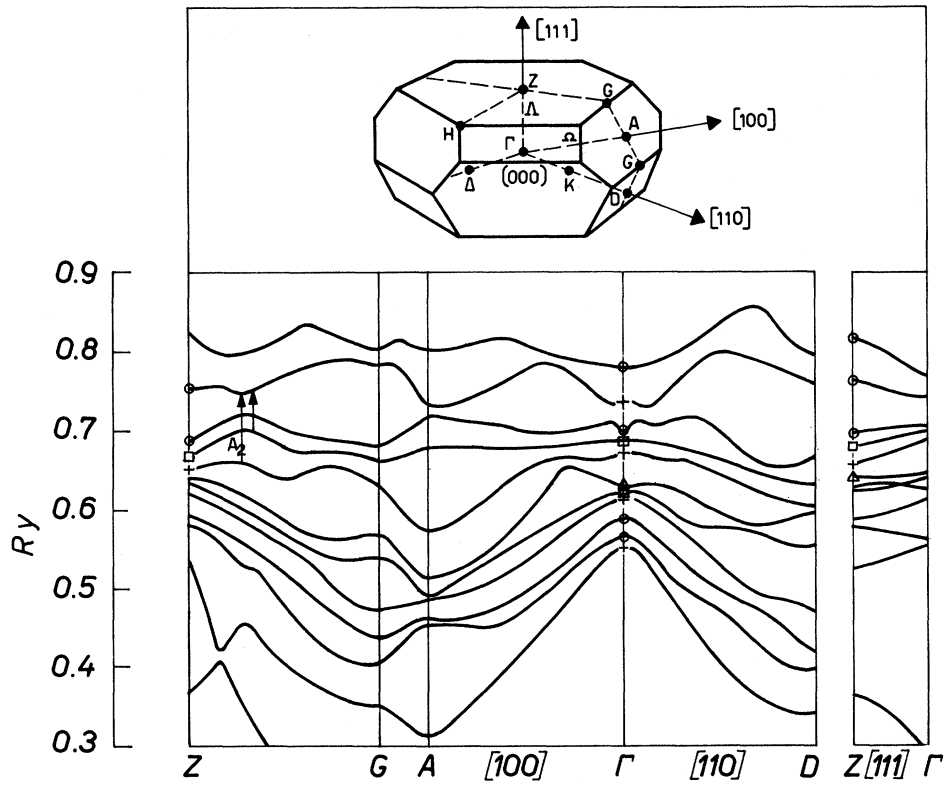

FIG. 8. The energy band structure of bismuth telluride (after Katsuki Ref. 8). The following symbols are used ○: Γ_6^+ or Z_6^+; Δ: $\Gamma_4^+ + \Gamma_5^+$ or $Z_4^+ + Z_5^+$; +: Γ_0^- or Z_6^-; □: $\Gamma_4^- + \Gamma_5^-$ or $Z_4^- + Z_5^-$.

s-like valence states increases more than that of p-like states and this results in the larger energy shifts of the high-energy transitions.

The band structure of bismuth telluride calculated by Katsuki, [8] on which we base our discussion, is reproduced in Fig. 8 together with a sketch of the Brillouin zone. The calculation has been carried out for the main symmetry directions [100], [110], and [111], and also for various other directions on the boundaries of the zone. We will restrict our following assignments to the first transitions listed in Table I.

The smaller energy gap is found at 0.11 eV between the top of the valence band at A and the bottom of the conduction band at M, and not at $k=0$. The indirect optical transitions occurring at 0.145 eV connect these two points of k space. The broad structure at 0.4 eV is assigned to the cluster of transitions taking place in the range 0.3–0.5 eV near Γ, while the small shoulder at 0.7 eV, [3] not reported in Table I, could be due to transitions between $Z_4^- + Z_5^-$ and Z_6^- near Z in the GZ direction. At the same point of the Brillouin zone, but starting from a lower valence band, we place the A_2 transition $Z_6^- \rightarrow Z_6^+$ allowed for both polarizations of light. According to Fig. 8, the conduction band probably has a saddle-point type of structure here, since the energy difference between the valence and the conduction bands increases when moving in the GZ direction and decreases in the [111] direction. It should be noted from Fig. 7 that n_{eff} reaches a value of four or five electrons at this energy, as one expects when the second or third valence bands participate in the transitions. The A_3 transition at 1.76 eV, which has a definite polarization dependence, probably occurs at point Γ as $\Gamma_4^+ + \Gamma_5^+ \rightarrow \Gamma_6^-$. The next threshold, on the contrary, is allowed for both polarizations and is likely to take place at Γ as $\Gamma_6^+ \rightarrow \Gamma_6^-$ and/or $\Gamma_6^- \rightarrow \Gamma_6^+$. Both the small reduced effective mass and the large relaxation constant (600 meV) found for this transition favor this assignment.

The next two transitions (E_3 and A_7' in Table I) at high energies are difficult to place on the same grounds, although we feel that both the effective number of electrons and the small lifetime suggest transitions to conduction bands starting from deeper valence states. The band scheme offers a number of possibilities along the [110] or [100] directions or at zone boundaries. We realize that this assignment is only tentative but a more precise and complete understanding of all transitions of bismuth telluride, including those of the second group, must wait until a direct evaluation of the imaginary part of the dielectric constant becomes available.

VI. CONCLUSIONS

The optical transitions of bismuth telluride in the visible and near uv range have been investigated by ER measurements at room temperature. Critical points have been identified through a quantitative line-shape analysis, by assuming that the optical field effects were due to strongly lifetime-broadened Franz-Keldysh tunneling. The dependence of the line shape upon the polarization of the light yielded an independent confirmation of their nature and allowed clarification of their anisotropic character. The peaks A_2, A_3, and $A_{4,5}$ of the reflectance spectra have been associated with two M_1 longitudinal saddle-point edges and an M_0 threshold at the center of the Brillouin zone. The A_3 line shows a strong dependence on the polarization in contrast with the other two transitions. On the basis of the available band structure these transitions have been correlated to cp within the Brillouin zone. Additional investigations, extended to the vacuum uv region, in conjunction with more refined theoretical calculations, should certainly provide a firmer basis towards the understanding of the electronic band structure of this compound.

ACKNOWLEDGMENTS

The authors are grateful to Professor R. Ricamo for his kind interest and to Dr. M. Piacentini for helpful discussions.

*Research done at the Physics Department of the University of Aquila, Aquila, Italy with the support of the Consiglio Nazionale delle Ricerche through the G.N.S.M.

[1]P. M. Lee and L. Pincherle, Proc. Phys. Soc. (London) 81, 361 (1963).

[2]F. Borghese and E. Donato, Nuovo Cimento 53B, 283 (1968).

[3]D. L. Greenaway and G. Harbeke, J. Phys. Chem. Solids 26, 1585 (1965).

[4]J. R. Drabble and R. Wolfe, Proc. Phys. Soc. (London) 69B, 1101 (1956).

[5]For a review of the experimental results before 1963 see also J. R. Drabble, in *Progress in Semiconductors*, edited by A. F. Gibson and R. E. Burgess (Wiley, New York, 1963), Vol. 7, p. 45.

[6]H. J. Goldsmid, Proc. Phys. Soc. (London) 72, 545 (1959).

[7]B. A. Efimova, I. Ya. Korenblum, V. I. Novikov, and and A. G. Ostroumov, Fiz. Tverd. Tela 3, 2746 (1961) [Soviet Phys. Solid State 3, 2004 (1962)].

[8]S. Katsuki, J. Phys. Soc. Japan 26, 58 (1969).

[9]I. G. Austin, Proc. Phys. Soc. (London) 76, 169 (1960).

[10]U. Hubner, Z. Naturforsch. 22A, 2086 (1967).

[11]V. V. Sobolev, S. D. Shutov, Yu. V. Popov, and S. N. Shestatskii, Phys. Status Solidi 30, 349 (1968).

[12]R. A. Smith, *Semiconductors* (Cambridge U. P., Cambridge, England, 1959), p. 172.

[13]This value is in good agreement with that determined from the resistivity by using a hole mobility $\mu_h = 400$ cm^2 V^{-1}sec^{-1} [see J. Black, E. M. Conwell, L. Seigle, and C. W. Spencer, J. Phys. Chem. Solids 2, 240 (1957)].

[14]T. C. Harman, S. E. Miller, and H. L. Goering, J. Phys. Chem. Solids 2, 181 (1957).

[15]K. L. Shaklee, F. H. Pollak, and M. Cardona, Phys. Rev. Letters 15, 883 (1965).

[16]Preliminary results have already been presented [A. Balzarotti and P. Picozzi, Bull. Ital. Phys. Soc. 62, 83 (1968)].

[17]D. E. Aspnes and A. Frova, Solid State Commun. 7, 155 (1969).

[18]J. Feinleib, Phys. Rev. Letters 16, 1200 (1966).

[19]The reflectivity data were extrapolated to infinite energies by assuming a tail function $R = c(\hbar\omega)^{-\gamma}$ and γ was determined such that the phase angle $\chi = 0$ below the absorption edge [see, e.g., W. J. Scouler, Phys. Rev. 178, A1353 (1969)]. A value of $\gamma = 3.9$ was found to hold for the data of Ref. 11.

[20]I. G. Austin, Proc. Phys. Soc. (London) 72, 545 (1958).

[21]J. E. Fischer and B. O. Seraphin, Solid State Commun. 5, 973 (1967).

[22]F. Lukes, data cited in Ref. 21.

[23]S. Ballarò, A. Balzarotti, and V. Grasso, Phys. Status Solidi 28, K109 (1968).

[24]A. Balzarotti and M. Grandolfo, Solid State Commun. 6, 815 (1968).

[25]E. Schmidt and W. H. Knausenberger, J. Opt. Soc. Am. 59, 857 (1969).

[26]In the 1–3 eV region the pseudo-Brewster angle of Bi_2Te_3 was calculated by differentiating the Fresnel formula for R_p with respect to the angle of incidence. The values of φ_B range from about 74° at 3 eV to 84° at 1.0 eV. The introduction of the refractive index of the first medium ($n = 1.33$) moves φ_B to low energies of $\sim 4°$ in this energy range.

[27]D. E. Aspnes and M. Cardona, Phys. Rev. 173, 714 (1968).

[28]A. Frova, P. J. Boddy, and Y. S. Chen, Phys. Rev. 157, 700 (1967).

[29]D. E. Aspnes, Phys. Rev. 153, A972 (1967).

[30]D. L. Greenaway, G. Harbeke, F. Bassani, and E. Tosatti, Phys. Rev. 178, 1340 (1969).

[31]Around 2.5 eV the effect of a strong anisotropy along the c axis of the optical constants on the R_p reflectance is to increase φ_B by about 3° and to enhance R_p by less than 5% for $\varphi < \varphi_B$ with respect to the isotropic case.

[32]M. Cardona and D. L. Greenaway, Phys. Rev. 133, A1685 (1964).

PHYSICAL REVIEW B VOLUME 3, NUMBER 4 15 FEBRUARY 1971

Diffuse X-Ray Scattering in Fast-Neutron-Irradiated Copper Crystals*

J. E. Thomas,† T. O. Baldwin,‡ and P. H. Dederichs§
Solid State Division, Oak Ridge National Laboratory, Oak Ridge, Tennessee 37830
(Received 15 June 1970)

Nearly perfect copper crystals with dislocation densities less than $\sim 10^3$/cm^2 have been irradiated with fast neutrons at doses up to 4×10^{19}/cm^2, and the diffuse x-ray scattering resulting from the defects produced has been studied in a variety of situations. Measurements were made with a double-crystal spectrometer to allow observations of the scattering very close (~ seconds of arc) to the Bragg peaks, for which a theoretical analysis of the data can be made. The diffuse scattering can be explained as resulting from defect clusters or dislocation loops ~ 100 Å in diam; there is an asymmetry of the diffuse scattering which appears to result from a predominance of large interstitial loops. This interpretation is consistent with electron-microscopy observations on these crystals. Diffuse scattering observations as well as anomalous x-ray transmission studies on irradiated crystals are suggested as very valuable tools to study the possibility of clustering phenomena in the annealing stages of various irradiated crystals.

INTRODUCTION

The irradiation of metal crystals is known to have marked effects on their physical properties. However, with the exception of lattice parameter measurements, little is known in a quantitative sense about the effects of irradiation on x-ray-diffraction properties. Although several years ago it was predicted that irradiation ought to cause strong diffuse scattering, [1] few observations of this scattering were made until quite recently in diamond, [2] copper, [3] silicon, [4] LiF, [5] BeO, [6] etc.

Diffuse x-ray scattering caused by the strains associated with radiation-induced defects in metals is quite difficult to observe for several reasons: (i) The diffuse scattering from point defects should be relatively weak for concentrations less than $\sim 10^{19}$/cm^3. If point defects are formed, as from electron irradiation, these defects are usually free to migrate at room temperature; hence, large doses of electron irradiation would be necessary at low temperatures to see the effects with conventional x-ray-diffraction apparatus (see, e.g., Simmons and Balluffi[7]); (ii) If clusters of defects